Vilnius
University
Press

Dynamics analysis of a nonlinear controlled predator–prey model with complex Poincaré map[*]

Huidong Cheng[a,b] [iD], **Xin Zhang**[b], **Tonghua Zhang**[c], **Jingli Fu**[d]

[a]College of Information and Control Engineering,
Shandong Foreign Affairs Vocational University,
Weihai 264504, China
chd900517@sdust.edu.cn

[b]College of Mathematics and System Sciences,
Shandong University of Science and Technology,
Qingdao 266590, China

[c]Department of Mathematics,
Swinburne University of Technology,
Hawthorn VIC 3122, Australia

[d]Institute of Mathematical Physics,
Zhejiang Sci-Tech University,
Hangzhou 310018, China
sqfujingli@163.com

Abstract. In this paper, we propose a class of predator–prey models with nonlinear state-dependent feedback control in the saturated state. The nonlinear state impulse control leads to a diversity of pulse and phase sets such that the Poincaré map built on the corresponding phase sets behaves like the single-peak function and multi-peak function with multiple discontinuities. We start our study by analyzing the exact pulse and phase sets of models under various cases generated by the dependent parameter space of nonlinear state feedback control, then construct the Poincaré map that is followed by investigating their monotonicity, continuity, concavity, and immobility properties. We also explore the existence, uniqueness, and sufficient conditions for the global stability of the order-1 periodic solutions of the systems. Numerical simulations are carried out to illustrate and reveal the biological significance of our theoretical findings.

Keywords: nonlinear feedback control, precise pulse and phase set, periodic solution, Poincaré map.

1 Introduction and model formulation

In recent years, predator–prey model research has been widely developed [4, 6, 9, 21], pulsed semicontinuous dynamical systems can solve various biological problems in

---

reality, such as control of biological resources [18], integrated pest management [11, 14, 16], marine fisheries fishing strategies [1, 3]. The study of pulsed semicontinuous dynamical systems has not only theoretical values but also practical significance by establishing pulsed differential equations that meet practical significance and studying their dynamical properties to reveal the biological laws involved.

State-dependent impulsive differential equations are well able to analyze and study threshold control strategies, and their qualitative theory and methods have been widely developed [2, 8, 19, 22]. For example, Liu [10] constructed a state feedback control predator–feeder model with Holling-II class and proved properties such as the existence and attractiveness of the system's order-1 periodic solution. In the article [5], a pulsed semidynamical system based on state feedback control of algal biomass was proposed, and the existence and stability of the order-1 periodic solution were investigated. Huang [7] proposed a model for pulsed injection of type I and type II diabetic insulin and analytically demonstrated the existence and local stability of the order-1 periodic solution. The dynamic properties of a mathematical accumulator model with state feedback control were investigated in the literature [13], and the results showed that pulses complicate the dynamic behavior. Nie [12] proposed a Lotka–Volterra predation model with state-dependent pulse effects and proved sufficient conditions for the existence and stability of semitrivial and positive periodic solutions of the system. Tang [20] developed a pulse culture-controlled plant disease model and analyzed the stability of the periodic solutions. Sun in the literature [17] proposed a model for the linear pulse-controlled differential equation:

$$
\left.\begin{aligned}
\frac{\mathrm{d}w(t)}{\mathrm{d}t} &= rw(t)\left(1 - \frac{w(t)}{K}\right) - bw(t)g(t), \\
\frac{\mathrm{d}g(t)}{\mathrm{d}t} &= g(t)\left(\frac{kbw(t)}{1 + bhw(t)} - d\right)
\end{aligned}\right\} \quad w(t) < ET,
$$

$$
\left.\begin{aligned}
\Delta w &= -p(w)w(t), \\
\Delta g &= -q(w)g(t) + \tau(g)
\end{aligned}\right\} \quad w(t) = ET, \ g(t) \leqslant \overline{g}_{ET},
$$

(1)

r, K, b, k, d are positive and satisfy $0 \leqslant h < k/d$ and

$$
K > \overline{K} \triangleq \frac{d + \sqrt{d^2 + rkd/(k - hd)}}{2b(k - hd)},
$$

where $w(t)$, $g(t)$ represent the population density of the prey and predator. Assuming that there are no predators, the per capita growth of food bait is $g(w) = r(1 - w(t)/K)$ with r representing the endogenous growth rate of the prey population, and K is the environmental carrying capacity. b represents the predation coefficient, and the density of the predator depends linearly on the density of the predator and prey, which is $bw(t)g(t)$. Assume that f is the conversion rate per capita from prey to predator in a saturated state and is defined by $f = kbw(t)/(1 + bhw(t))$, where $0 < k < 1$ is the conversion factor. Functions $p(w)$, $q(w)$ are linear.

In the literature [17], a predator–prey model for integrated pest management was proposed in which the release rate of predators and the lethality of prey were linear,

which assumes that resources such as labor, equipment, and costs are adequate. In reality, resources are limited, and if these resources change, it will cause changes in population density. However, resource change is a dynamic process that changes over time, so studying resource limitation models can better manage and protect populations [15]. For this purpose, we consider using nonlinear control functions $\alpha(w, g) = -\sigma w/(w + m)$ and $\beta(w, g) = \tau/(1 + \theta g)$. That means that both the prey lethality and the number of released predators depend on their densities. Therefore, we propose a predator–prey model with nonlinear state-dependent feedback control with limited resource saturation:

$$
\left.
\begin{aligned}
\frac{\mathrm{d}w(t)}{\mathrm{d}t} &= rw(t)\left(1 - \frac{w(t)}{K}\right) - bw(t)g(t), \\
\frac{\mathrm{d}g(t)}{\mathrm{d}t} &= g(t)\left(\frac{kbw(t)}{1 + bhw(t)} - d\right)
\end{aligned}
\right\} \quad w(t) \neq ET,
$$

$$
\left.
\begin{aligned}
w(t^+) &= \left[1 - \frac{\sigma w(t)}{w(t) + m}\right]w(t), \\
g(t^+) &= g(t) + \frac{\tau}{1 + \theta g(t)}
\end{aligned}
\right\} \quad w(t) = ET.
$$

(2)

In the model, $0 < \sigma < 1$, $m \geqslant 0$ denote the maximum lethality and half-saturation constants of the prey-eating population, respectively. $\tau \geqslant 0$ denotes the predator release, and $\theta \geqslant 0$ denotes the shape parameter. When the prey population density reaches the economic threshold (ET), pulse control is performed to reduce the prey population density to $(1 - \sigma ET/(ET + m))ET$ and increase the predator population density to $g(t) + \tau/(1 + \theta g(t))$. In particular, when $m = 0$, $\theta = 0$ is satisfied. System (2) becomes a control model (1) with linear state feedback.

To facilitate the discussion of the exact pulse and phase set, we consider the properties of the state feedback function $f(g) = g + \tau/(1 + \theta g)$. It is easy to know that it has an asymptote $g = -1/\theta$, and there exists a positive minimal point $g_m = (\sqrt{\theta\tau} - 1)/\theta$ when $\theta\tau > 1$. Therefore, when $g < g_m$ ($g > g_m$), $f(g)$ is decreasing (increasing). When $\theta\tau > 1$, $f(g_m) = (\sqrt{\theta\tau} - 1)/\theta + \tau/(1 + \sqrt{\theta\tau}) < \tau$, $f(0) = \tau > f(g_m)$.

The following discusses the nature of system (2) in the absence of pulse control:

$$
\begin{aligned}
\frac{\mathrm{d}w}{\mathrm{d}t} &= rw\left(1 - \frac{w}{K}\right) - bwg \triangleq Q(w, g), \\
\frac{\mathrm{d}g}{\mathrm{d}t} &= g\left(\frac{kbw}{1 + bhw} - d\right) \triangleq P(w, g).
\end{aligned}
$$

(3)

The two isoclines of system (3) are

$$
L_1: w = \frac{d}{b(k - hd)} \quad \text{and} \quad L_2: g = \frac{r}{b}\left(1 - \frac{g}{K}\right).
$$

System (3) has three equilibrium points: $0(0, 0)$, $K(K, 0)$, and $E^*(w^*, g^*)$ with

$$
w^* = \frac{d}{b(k - hd)}, \qquad g^* = \frac{r}{b} - \frac{rd}{b^2(k - hd)K}.
$$

Let

$$\Delta = A^2 - 4B, \qquad A = \frac{3rd\lambda}{kb(k-hd)} - d, \qquad B = \frac{rbd(k-hd) - krd^2}{bhK} - \frac{3rd^2}{Kb(k-hd)}.$$

Lemma 1. *The equilibrium points $0(0,0)$ and $K(K,0)$ are saddle points of system* (3), *and $E^*(w^*, g^*)$ is a global asymptotically stable node or focus of system* (3). *We have*:

   (I) *When $bkK - bhdK - d < 0$, there is no positive equilibrium point, and $K(K,0)$ is globally stable.*

  (II) *When $bkK - bhdK - d > 0$, $B > 0$, $\Delta > 0$, $E^*(w^*, g^*)$ is a focal point.*

 (III) *When $bkK - bhdK - d > 0$, $B > 0$, $\Delta > 0$, $E^*(w^*, g^*)$ is a node.*

Sun [17] discussed the existence, stability, and other dynamical properties of the order-1 periodic solution under the condition of case (I) in Lemma 1 by the method of the successor function. However, the properties under case (II) have not been solved. We will use the Poincaré map, a tool to perform a more comprehensive study of the nonlinear state feedback dynamics properties of case (II). The following discussion in this paper holds under condition $bkK - bhdK - d > 0$, $B > 0$, $\Delta < 0$ if not otherwise stated.

Section 2 of the paper provides a discussion of the exact pulse and phase set resulting from the dependent parameters due to nonlinear pulse control. Section 3 investigates the properties of the Poincaré map in different cases and proves the existence, uniqueness, and stability of the order-1 periodic solution. Finally, in Section 4, our results are illustrated by numerical simulations, and the biological implications of the findings are given.

2   Construction of the Poincaré map

2.1   Exact pulse and phase set

From system (2) let the line $EP = (1 - \sigma ET/(ET + h))ET$ in the plane. We discuss the following three cases according to the position relationships between ET, EP, and w^*:

  (a) $0 \leqslant EP < w^* < ET$;

  (b) $0 \leqslant EP < ET \leqslant w^*$;

  (c) $w^* < EP$.

Based on the biological significance, $ET < K$ and $R_+^2 = \{(w, g)\colon w \geqslant 0, g \geqslant 0\}$ are assumed in this paper. For case (a), when $ET > w^*$ defines the line L_3: $w = ET$, L_4: $w = EP$ in the plane, let the intersection of lines L_2 and L_3 be $T(ET, g_T)$. There exists a solution curve Γ_1 tangent to line L_3 at point $T(ET, g_T)$. Denote the point where Γ_1 intersects with line L_2 by $C(w_c, g_c)$. Then, depending on the position of point $C(w_c, g_c)$ to line L_4, one obtains the following two cases to discuss:

  Case 1. When $EP < w_c$, Γ_1 does not intersect with L_4 (as shown in Fig. 1(a));

  Case 2. When $EP \geqslant w_c$, Γ_1 intersects with L_4 (as shown in Fig. 1(b)).

For case 1, that is, when $EP < w_c$, Γ_1 does not intersect with line L_4, denote the intersection of lines L_2 and L_4 by $P(EP, g_p)$. There exists a solution curve Γ_2 tangent to L_4 at point $P(EP, g_p)$. In addition, Γ_2 intersects L_3 at point $A(ET, g_A)$. It is known from
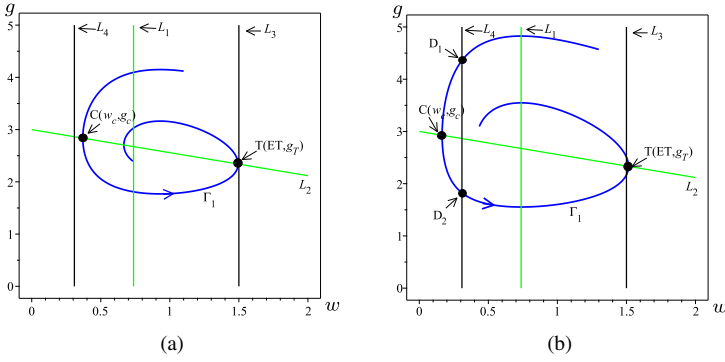
Figure 1. The relationship between Γ_1 and L_4, where the parameters for $EP < w_c$ and $EP \geqslant w_c$ are: (a) $r = 1.5$, $K = 6.8$, $ET = 1.5$, $b = 0.5$, $k = 0.9$, $h = 0.1$, $d = 0.4$, $\sigma = 0.9$, $m = 0.2$; (b) $d = 0.32$.
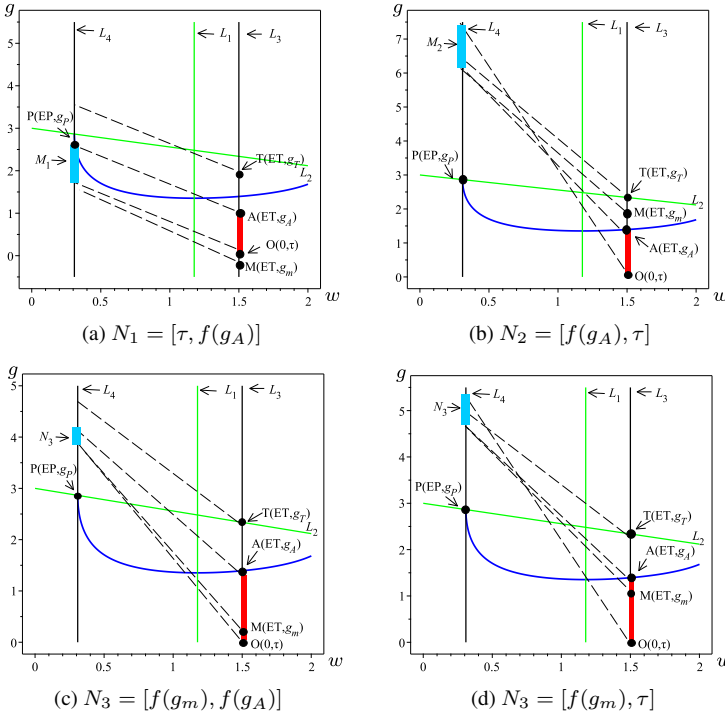

Figure 2. When $bkK - bhdK - d > 0$, $ET \leqslant w^*$, images of the pulse and phase set with parameters as: (a) $r = 1.5$, $K = 6.8$, $ET = 1.5$, $b = 0.5$, $k = 0.9$, $h = 0.1$, $d = 0.5$, $\sigma = 0.9$, $m = 0.2$, $\tau = 2$, $\theta = 0.4$; (b) $\tau = 7$, $\theta = 0.4$; (c) $\tau = 4$, $\theta = 0.3$; (d) $\tau = 5$, $\theta = 0.5$.

the above analysis that the pulse set is: $M_1 = \{(w, g) \in \mathbb{R}^2 \colon w = ET, 0 \leqslant g \leqslant g_A\}$. Based on the different positions of the minimal value point g_m on the pulse set, we can get the corresponding phase set as shown in Fig. 2.

When $\theta\tau \leqslant 1$, $g_m \leqslant 0$,

$$\ell_{11} = \{(w(t^+), g(t^+)) \in \mathbb{R}^2 : w(t^+) = EP, \, g(t^+) \in N_1\}.$$

When $\theta\tau > 1$, $g_A \leqslant g_m$,

$$\ell_{12} = \{(w(t^+), g(t^+)) \in \mathbb{R}^2 : w(t^+) = EP, \, g(t^+) \in N_2\}.$$

When $\theta\tau > 1$, $g_A > g_m$,

$$\ell_{13} = \{(w(t^+), g(t^+)) \in \mathbb{R}^2 : w(t^+) = EP, \, g(t^+) \in N_3\}.$$

Here

$$N_1 = [\tau, f(g_A)], \qquad N_2 = [f(g_A), \tau], \qquad N_3 = [f(g_m), \max\{\tau, f(g_A)\}].$$

For case 2, when $EP \geqslant w_c$, Γ_1, which passes through point $T(ET, g_T)$ and is tangent to L_3, intersects L_4 at two points $D_1(EP, g_{T_1}^+)$ and $D_2(EP, g_{T_2}^+)$. It is easily known that the trajectory starting from any point (EP, g^+) (here $g_{T_1}^+ < g^+ < g_{T_2}^+$) will be unaffected by the pulse. In this case, the pulse set is $M_2 = \{(w, g) \in \mathbb{R}^2 : w = ET, \, 0 \leqslant g \leqslant g_T\}$. The phase set is shown in Fig. 3.
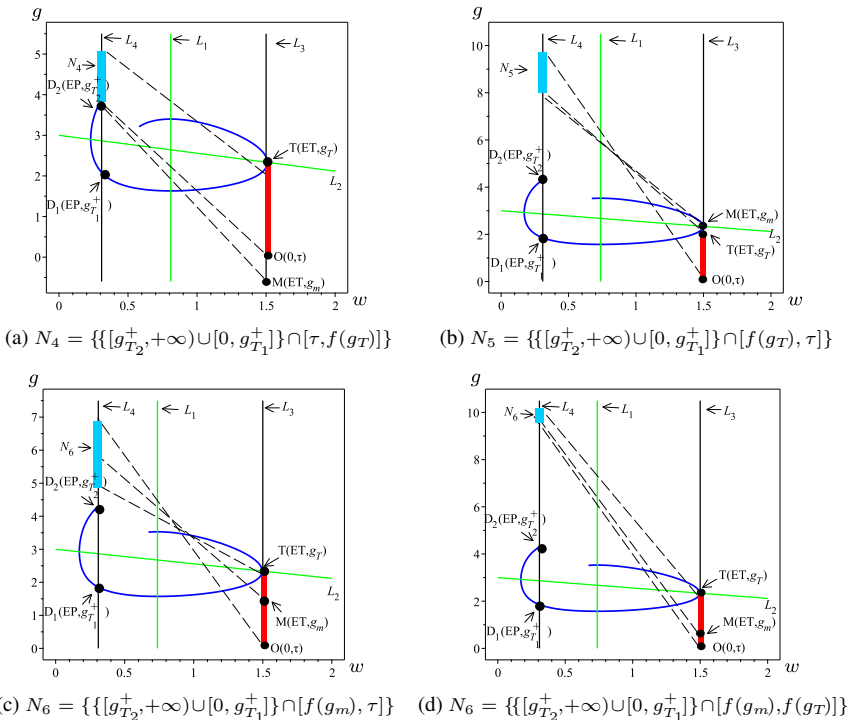

Figure 3. When $EP \geqslant w_c$, images of the pulse and phase set with parameters as: (a) $r = 1.5$, $K = 6.8$, $ET = 1.5$, $b = 0.5$, $k = 0.9$, $h = 0.1$, $d = 0.5$, $\sigma = 0.9$, $m = 0.2$, $\tau = 2$, $\theta = 0.4$; (b) $\tau = 7$, $\theta = 0.4$; (c) $\tau = 4$, $\theta = 0.3$; (d) $\tau = 5$, $\theta = 0.5$.
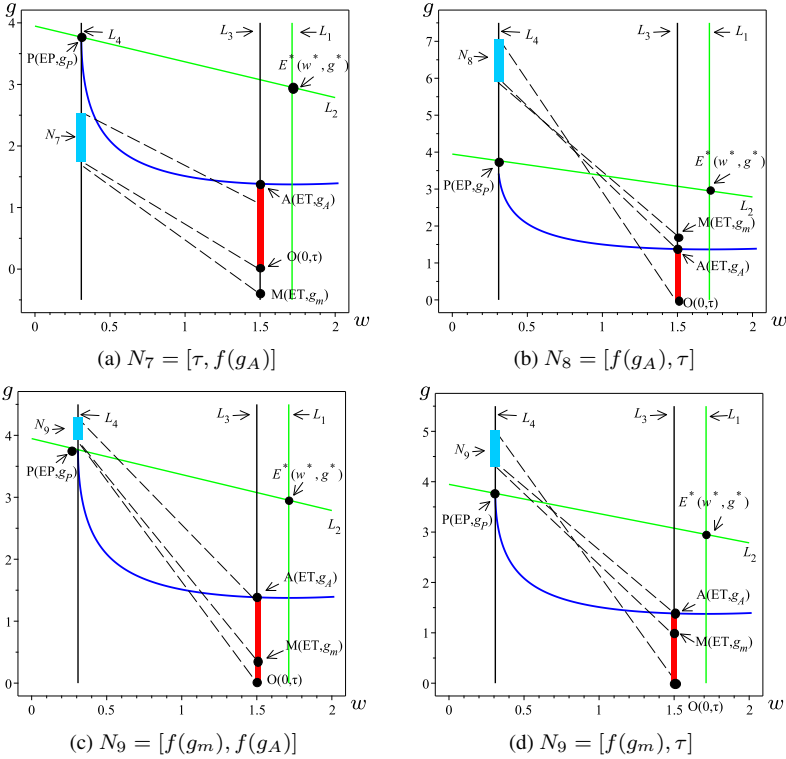
Figure 4. When $EP \geqslant 0$, $ET \leqslant w^*$, images of the pulse and phase set with parameters as: (a) $r = 1.5$, $K = 6.8$, $ET = 1.5$, $b = 0.38$, $k = 0.9$, $h = 0.1$, $d = 0.55$, $\sigma = 0.9$, $m = 0.2$, $\tau = 2$, $\theta = 0.4$; (b) $\tau = 7$, $\theta = 0.4$; (c) $\tau = 4$, $\theta = 0.3$; (d) $\tau = 5$, $\theta = 0.5$.

When $\theta\tau \leqslant 1$, $g_m \leqslant 0$,
$$\ell_{21} = \left\{ \left(w(t^+), g(t^+) \right) \in \mathbb{R}^2 \colon w(t^+) = EP, \ g(t^+) \in N_4 \right\}.$$

When $\theta\tau > 1$, $g_T \leqslant g_m$,
$$\ell_{22} = \left\{ \left(w(t^+), g(t^+) \right) \in \mathbb{R}^2 \colon w(t^+) = EP, \ g(t^+) \in N_5 \right\}.$$

When $\theta\tau > 1$, $g_T > g_m$,
$$\ell_{23} = \left\{ \left(w(t^+), g(t^+) \right) \in \mathbb{R}^2 \colon w(t^+) = EP, \ g(t^+) \in N_6 \right\}.$$

Here
$$N_4 = \left\{ \left\{ \left[g_{T_2}^+, +\infty \right) \cup \left[0, g_{T_1}^+ \right] \right\} \cap \left[\tau, f(g_T) \right] \right\},$$
$$N_5 = \left\{ \left\{ \left[g_{T_2}^+, +\infty \right) \cup \left[0, g_{T_1}^+ \right] \right\} \cap \left[f(g_T), \tau \right] \right\},$$
$$N_6 = \left\{ \left\{ \left[g_{T_2}^+, +\infty \right) \cup \left[0, g_{T_1}^+ \right] \right\} \cap \left[f(g_m), \max\{\tau, f(g_T)\} \right] \right\}.$$

For case (b), when $ET \leqslant w^*$, the equilibrium point is right of the pulse set. The pulse set is: $M_1 = \{(w,g) \in \mathbb{R}^2 \colon w = ET, 0 \leqslant g \leqslant g_A\}$, the phase set shown in Fig. 4.

(a) $N_{10} = \{\{[g_{T_2}^+, +\infty) \cup [0, g_{T_1}^+]\} \cap [\tau, f(g_T)]\}$

(b) $N_{11} = \{\{[g_{T_2}^+, +\infty) \cup [0, g_{T_1}^+]\} \cap [f(g_T), \tau]\}$

(c) $N_{12} = \{\{[g_{T_2}^+, +\infty) \cup [0, g_{T_1}^+]\} \cap [f(g_m), \tau]\}$

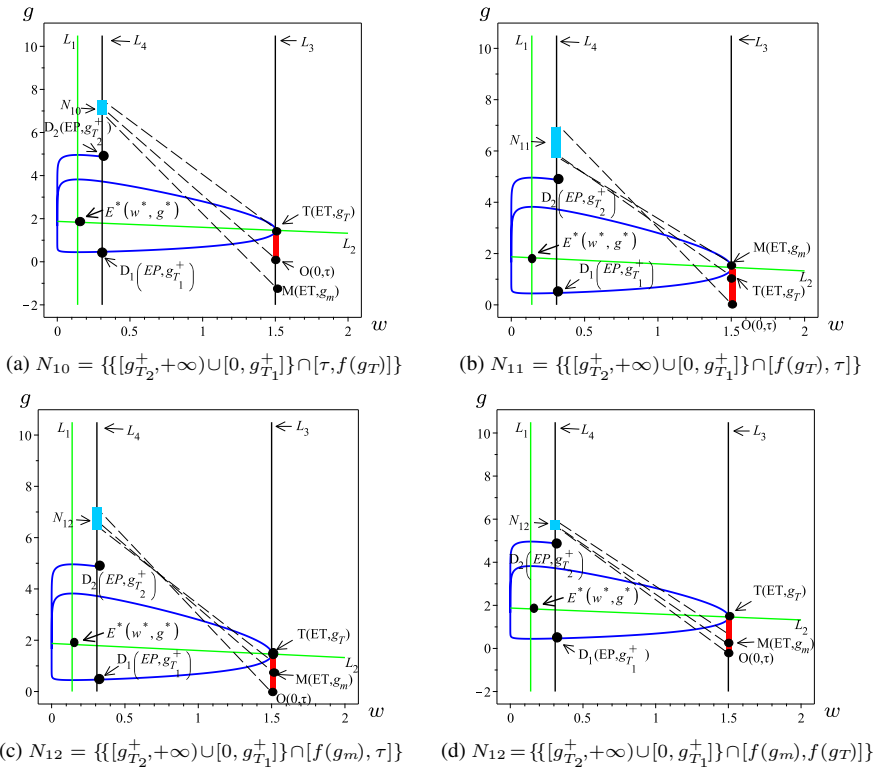(d) $N_{12} = \{\{[g_{T_2}^+, +\infty) \cup [0, g_{T_1}^+]\} \cap [f(g_m), f(g_T)]\}$

Figure 5. When $EP > w^*$, images of the pulse and phase set with parameters as: (a) $r = 1.5$, $K = 6.8$, $ET = 1.5$, $b = 0.8$, $k = 0.9$, $h = 0.1$, $d = 0.1$, $\sigma = 0.9$, $m = 0.2$, $\tau = 7$, $\theta = 0.1$; (b) $\tau = 7$, $\theta = 0.4$; (c) $\tau = 7$, $\theta = 0.2$; (d) $\tau = 4$, $\theta = 0.3$.

When $\theta\tau \leqslant 1, g_m \leqslant 0$,

$$\ell_{31} = \{(w(t^+), g(t^+)) \in \mathbb{R}^2 : w(t^+) = EP0, \ g(t^+) \in N_7\}.$$

When $\theta\tau > 1, g_A \leqslant g_m$,

$$\ell_{32} = \{(w(t^+), g(t^+)) \in \mathbb{R}^2 : w(t^+) = EP, \ g(t^+) \in N_8\}.$$

When $\theta\tau > 1, g_A > g_m$,

$$\ell_{33} = \{(w(t^+), g(t^+)) \in \mathbb{R}^2 : w(t^+) = EP, \ g(t^+) \in N_9\}.$$

Here

$$N_7 = [\tau, f(g_A)], \qquad N_8 = [f(g_A), \tau], \qquad N_9 = [f(g_m), \max\{\tau, f(g_A)\}].$$

For case (c), when $w^* < EP$ the equilibrium point is left of the phase set, we can obtain different phase sets. The pulse set is: $M_2 = \{(w, g) \in \mathbb{R}^2 : w = ET, \ 0 \leqslant g \leqslant g_T\}$, and the phase shown in Fig. 5.

$$N_{12} = \{\{[g_{T_2}^+, +\infty) \cup [0, g_{T_1}^+]\} \cap [f(g_m), f(g_T)]\}$$

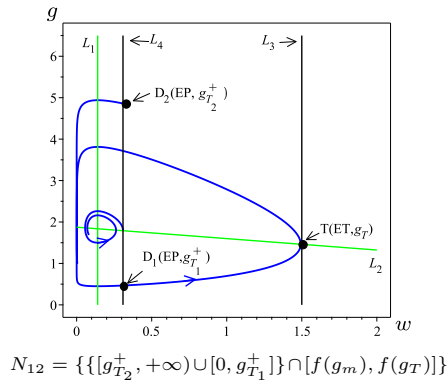**Figure 6.** When $EP > w^*$, images of the pulse and phase set with the same parameters as in Fig. 5.

When $\theta\tau \leqslant 1$, $g_m \leqslant 0$,

$$\ell_{41} = \{(w(t^+), g(t^+)) \in \mathbb{R}^2 : w(t^+) = EP, \, g(t^+) \in N_{10}\}.$$

When $\theta\tau > 1$, $g_T \leqslant g_m$,

$$\ell_{42} = \{(w(t^+), g(t^+)) \in \mathbb{R}^2 : w(t^+) = EP, \, g(t^+) \in N_{11}\}.$$

When $\theta\tau > 1$, $g_T > g_m$,

$$\ell_{43} = \{(w(t^+), g(t^+)) \in \mathbb{R}^2 : w(t^+) = EP, \, g(t^+) \in N_{12}\}.$$

Here

$$N_{10} = \{\{[g_{T_2}^+, +\infty] \cup [0, g_{T_1}^+]\} \cap [\tau, f(g_T)]\},$$
$$N_{11} = \{\{[g_{T_2}^+, +\infty] \cup [0, g_{T_1}^+]\} \cap [f(g_T), \tau]\},$$
$$N_{12} = \{\{[g_{T_2}^+, +\infty] \cup [0, g_{T_1}^+]\} \cap [f(g_m), \max\{\tau, f(g_T)\}]\}.$$

In this case, as shown in Fig. 6, the trajectory from any point (EP, g^+) (here $g^+ \in [g_{T_2}^+, +\infty] \cup [0, g_{T_1}^+])$ gradually approaches the equilibrium point E^* after finite pulses (or no pulses).

2.2 Definition of Poincaré map

Based on the above exact pulse and phase sets, this section defines the Poincaré map.

Let $S_{ET} = \{(w, g) : w = ET, \, g \geqslant 0\}$ and $S_{\sigma ET} = \{(w, g) : w = EP, \, g \geqslant 0\}$. The sets S_{ET} and $S_{\sigma ET}$ are part of the lines L_3: $w = ET$ and L_4: $w = EP$, respectively. Let the initial point $P_k^+(EP, g_k^+) \in S_{\sigma ET}$ and the trajectory over point $P_k^+(EP, g_k^+)$ reach point $P_{k+1}(ET, g_{k+1}) \in S_{ET}$. From the equations of system (2) it follows that the value of g_{k+1} depends on the size of g_k^+, which we set as $g_{k+1} = \rho g_k^+$. After the action of the pulse, the trajectory finally intersects the line L_4 at the point $P_{k+1}^+(EP, g_{k+1}^+)$, where $g_{k+1}^+ = g_{k+1} + \tau/(1 + \theta g_{k+1})$. We only focus on the following areas:

$$\Omega_1 = \left\{(w, g) : w > 0, \, g > 0, \, g < \frac{r(K - w)}{kb}\right\}.$$

Based on the above analysis, the Poincaré map is as follows:

$$g_{k+1}^+ = g_{k+1} + \frac{\tau}{1 + \theta g_{k+1}} = \rho(g_k^+) + \frac{\tau}{1 + \theta \rho(g_k^+)} \triangleq P_M(g_k^+). \tag{4}$$

Define

$$\frac{\mathrm{d}g}{\mathrm{d}w} = \frac{P(w,g)}{Q(w,g)} = \frac{gK(kbw - d - bdhw)}{w(1 + bhw)(rK - rw - bgK)} \triangleq G(w,g), \tag{5}$$
$$g(EP) = g_0^+.$$

Then system (2) is transformed into

$$g(w) = g(w; (EP, S)) \triangleq g(w, S).$$

Here $EP \leqslant w \leqslant ET$, $S \in \ell_{ij}$ ($i = 1, 2, 3, 4$; $j = 1, 2, 3$).

For model (5), one can obtain

$$g(w, S) = S + \int_{EP}^{w} G(s, g(s, S)) \, \mathrm{d}s.$$

The Poincaré map P_M on region Ω_1 takes this form:

$$P_M(S) = g(ET, S) + \frac{\tau}{1 + \theta g(ET, S)}.$$

3 Dynamical properties of system (2)

Bellow we discuss the properties of P_M in case 1 and obtain the following result.

Theorem 1. *When $EP < w_c$ and $\theta\tau \leqslant 1$, P_M has the following properties (as shown in Fig. 7(a)):*

(I) *The domain and range of P_M are $[0, +\infty)$ and N_1, respectively. g_p is an extreme point of P_M, and P_M increases on $[0, g_p]$ and decreases on $[g_p, +\infty)$, respectively. Furthermore, P_M is continuously differentiable over its domain and, when P_M holds on the interval $(0, g_p]$ with $\mathrm{d}P_M^2(S)/\mathrm{d}S^2 < 0$, P_M is concave on the interval $(0, g_p]$. When $g_k^+ \to +\infty$, there exists a horizontal asymptote $g = \tau$ for P_M. The maximum value of P_M is $P_M(g_p)$, and the minimum value is τ.*

(II) *P_M has at least one fixed point. Especially, suppose the fixed point $\widetilde{g}$ is unique when $\widetilde{g} \in [g_p, +\infty) \cap N_1$, $P_M(g_p) \geqslant g_p$. Then $\widetilde{g}$ is globally stable. When $P_M(g_p) \leqslant g_p$, $\widetilde{g} \in [0, g_p] \cap N_1$, the sufficient condition for the global stability of the order-1 periodic solution is $P_M^2(g^+) > g^+$ for all $g^+ \in [g_p, \widetilde{g})$.*

Proof. (I) Take a point P_k^+ from the set of pulses M_1, its trajectory passes through the pulses to reach the phase set N_1. In this case, an infinite number of pulses are experienced, so the domain of P_M is $[0, +\infty)$.
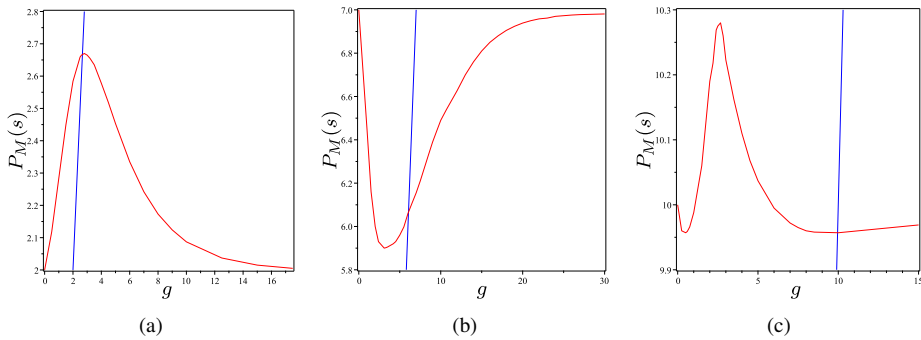
Figure 7. When $bkK - bhdK - d > 0$, $ET \leqslant w^*$, the image of P_M with parameters as: (a) $r = 1.5$, $K = 6.8$, $ET = 1.5$, $b = 0.5$, $k = 0.9$, $h = 0.1$, $d = 0.5$, $\sigma = 0.9$, $m = 0.2$, $\tau = 2$, $\theta = 0.4$; (b) $\tau = 7$, $\theta = 0.4$, (c) $\tau = 10$, $\theta = 0.11$.

For any points $P_{p_1}^+(EP, g_{p_1}^+)$, $P_{p_2}^+(EP, g_{p_2}^+)$, here $g_{p_1}^+, g_{p_2}^+ \in [0, g_p]$, let $g_{p_1}^+ < g_{p_2}^+$ and $g_{p_1+1} = \rho(g_p^+)$, $g_{p_1+1} < g_{p_2+1}$ can be obtained from the theorem. After pulse, we can get

$$
\begin{aligned}
P_M(g_{p_1}^+) &= g(ET, g_{p_1+1}) + \frac{\tau}{1 + \theta g(ET, g_{p_1+1})} \\
&< g(ET, g_{p_2+1}) + \frac{\tau}{1 + \theta g(ET, g_{p_2+1})} \\
&= P_M(g_{p_2}^+),
\end{aligned}
$$

so P_M is increasing on $[0, g_p]$.

For any points $Q_{q_1}^+(EP, g_{q_1}^+)$, $Q_{q_2}^+(EP, g_{q_2}^+)$, satisfying $g_{q_1}^+, g_{q_2}^+ \in [g_p, +\infty)$, let $g_{q_1}^+ < g_{q_2}^+$. The trajectory passing the initial point either $Q_{q_1}^+$ or $Q_{q_2}^+$ crosses N_1 once before reaching M_1, indicating that the coordinates of the two tracks intersecting N_1 are $Q_{k_1}^+(EP, g_{k_1}^+)$, $Q_{k_2}^+(EP, g_{k_2}^+)$. Note that point $Q_{k_1}^+$ is above point $Q_{k_2}^+$ (so $g_{k_1}^+ > g_{k_2}^+$), and we obtain $P_M(g_{q_1}^+) = P_M(g_{k_1}^+) > P_M(g_{k_2}^+) = P_M(g_{q_2}^+)$, so P_M is decreasing on $[g_p, +\infty)$.

From model (2) we get that functions $P(w, g)$, $Q(w, g)$ are continuously differentiable in their domain. According to the Cauchy–Lipschitz theorem, P_M is continuously differentiable.

Using (5), we can get

$$
\begin{aligned}
\frac{\partial G}{\partial g} &= \frac{rK(K - w)(kbw - d - bdhw)}{w(1 + bhw)(rK - rw - bgK)^2}, \\
\frac{\partial^2 G}{\partial g^2} &= \frac{2rbK^2(kbw - d - bdhw)(K - w)}{w(1 + bhw)(rK - rw - bgK)^3}.
\end{aligned}
$$

When $w \leqslant ET < K$, there is $kbw - bdhw - d < 0$, which yields $kbw/(1 + bhw) - d < 0$, and when $g < g_p$, there is $rw(1 - w/K) - bwg > 0$; When $g > g_p$, there is $rw(1 - w/K) - bwg < 0$, so when $g < g_p$, we can get $\partial G/\partial g < 0$, $\partial^2 G/\partial g^2 < 0$.

From the Cauchy–Lipschitz theorem with parameters we can obtain the scalar differential equation

$$\frac{\partial g(w,S)}{\partial S} = \exp\left(\int\limits_{(1-\theta)ET}^{w} \frac{\partial}{\partial g}\frac{Q(z,v(z,S))}{P(z,v(z,S))}\,\mathrm{d}z\right) > 0,$$

$$\frac{\partial^2 g(w,S)}{\partial S^2} = \frac{\partial g(w,S)}{\partial S}\left(\int\limits_{(1-\theta)ET}^{w} \frac{\partial^2}{\partial g^2}\frac{Q(z,w(z,S))}{P(z,w(z,S))}\frac{\partial g(z,S)}{\partial S}\,\mathrm{d}z\right) < 0.$$

From the above analysis it follows that

$$\frac{\mathrm{d}P_M(S)}{\mathrm{d}S} = \frac{\mathrm{d}g(ET,S)}{\mathrm{d}S}\left[1 - \frac{\tau\theta}{(1+\theta g(ET,S))^2}\right],$$

$$\frac{\mathrm{d}P^2{}_M(S)}{\mathrm{d}S^2} = \frac{\mathrm{d}^2 g(ET,S)}{\mathrm{d}S^2}\left[1 - \frac{\tau\theta}{(1+\theta g(ET,S))^2}\right]$$
$$+ \left(\frac{\mathrm{d}g(ET,S)}{\mathrm{d}S}\right)^2 \frac{2\theta^2\tau}{(1+\theta g(ET,S))^3}.$$

Thus, when $S < g_p$ for all $g(ET,S)$, if $\theta\tau \leqslant 1$, then we have $\mathrm{d}P_M(S)/\mathrm{d}S > 0$. Note that in $\mathrm{d}P^2{}_M(S)/\mathrm{d}S^2$ the former term is positive, and the latter is negative, which means that the sign of $\mathrm{d}P^2{}_M(S)/\mathrm{d}S^2$ may change. Therefore, P_M is concave on the interval $(0, g_p)$ when P_M has $\mathrm{d}P^2{}_M(S)/\mathrm{d}S^2 < 0$ holding on the interval $(0, g_p)$.

Next, show that as g_k^+ increases, P_M converges to the asymptote $g = \tau$. Define Ω_1 as

$$\Omega_1 = \left\{(w,g)\colon w > 0,\ g > 0,\ g < \frac{r(K-w)}{bk}\right\}.$$

Since P_M is increasing on $[0, g_p]$ and decreasing on $[g_p, +\infty)$, Ω_1 is an invariant set of system (2). Let $L = g - r(K-w)/(bk)$. If $[P(w,g), Q(w,g)\cdot(r/(bk),1)]_{L=0} \leqslant 0$, where $\cdot$ represents the scalar product of vectors, then the vector field will eventually reach the boundary Ω_1. So Ω_1 is an invariant set, which can be calculated by $P_M(w)|_{L=0} \doteq [rw(1 - w/K) - bwg](r/bk + g(kbw/(1+bhw) - d)$.

Since P_M is increasing on $[0, g_p]$ and decreasing on $[g_p, +\infty)$, so for any $g_0^+ \in [0, g_p]$, $P_M(g_0^+)$ is bounded, and $P_M([g_p, +\infty)) \subset P_M([0, g_p])$. According to the Cauchy–Lipschitz theorem, g_{k+1} is determined by g_k^+ and can be expressed as $g_{k+1} = P_M(g_k^+)$. It is always $\mathrm{d}g/\mathrm{d}t < 0$ at any point on the phase set, therefore, $\lim_{g_k^+ \to \infty}\rho(g_k^+) = 0$. So $\lim_{g_k^+ \to \infty}P_M(g_k^+) = \lim_{g_k^+ \to \infty}(\rho(g_k^+) + \tau/(1+\theta\rho(g_k^+)) = \tau$. Therefore, as g_k^+ increases, P_M tends to the asymptote $g = \tau$ as shown in Fig. 7(a).

(II) First, prove that P_M has at least one fixed point.

P_M is decreasing on $[g_p, +\infty)$, so there exists a $\overline{g} \in [g_p, +\infty)$ such that $P_M(\overline{g}) < \overline{g}$. When $\tau > 0$, $P_M(0) = \tau > 0$, there must exist $\tau > 0$, $P_M(0) = \tau > 0$ such that $P_M(\widetilde{g}) = \widetilde{g}$, and there is at least one fixed point on the interval $[0, +\infty)$.

When $P_M(g_p) \leqslant g_p$, for all $g_k \in [g_p, +\infty)$, that P_M is decreasing on $[g_p, +\infty)$, yields $P_M(g_k) < P_M(g_p) < g_p < g_k$, so that P_M has no fixed point on $[g_p, +\infty)$. P_M is increasing on $[0, g_p]$, concave on $[0, g_p]$, and $P_M(0) > 0$. So there is at least one fixed point on the interval $[0, g_p]$.

When $P_M(g_p) \geqslant g_p$, P_M is increasing on $[0, g_p]$, concave on $[0, g_p]$, and $P_M(0) > 0$. It follows that P_M has no fixed point on $[0, g_p]$. P_M is decreasing on $[g_p, +\infty)$, so there is at least one fixed point on the interval $[g_p, +\infty)$.

The following evidence is sufficient. For all $g^+ \in (g_p, \widetilde{g})$, we note that after one pulse is $P_M(g^+) = g_1^+$ and after n pulses are $P_M^n(g^+) = g_n^+$. According to $g^+ \in (g_p, \widetilde{g})$, we have $g_p < g^+ < \widetilde{g}$, and according to the monotonicity of P_M, we obtain $P_M(g_p) > P_M(g^+) > P_M(\widetilde{g})$, which is $g_1^+ > \widetilde{g}$. Then after the pulse, there is $P_M(g_1^+) < P_M(\widetilde{g})$, which is $g_2^+ < \widetilde{g}$. After one more pulse, we get $P_M(g_2^+) > P_M(\widetilde{g})$, which is $g_3^+ > \widetilde{g}$. By mathematical induction we get $g_{2n}^+ \langle \widetilde{g}, g_{2n+1}^+ \rangle \widetilde{g}$, $n = 0, 1, 2, \ldots$.

For all $g^+ \in [g_p, \widetilde{g})$, $P_M^2(g^+) > g^+$, that is, $g^+ < g_2^+ < \widetilde{g}$. According to the above analysis, we can get $g_1^+ > P_M(g_1^+) > P_M(g_2^+) = g_3^+$, so we can get $\widetilde{g} < g_3^+ < g_1^+$.

To summarize, we can obtain $g^+ < g_2^+ < \widetilde{g} < g_3^+ < g_1^+$. After one pulse there is $g^+ < g_2^+ < g_4^+ < \widetilde{g} < g_5^+ < g_3^+ < g_1^+$. From mathematical induction we get $g^+ < g_2^+ < \cdots < g_{2n}^+ < \widetilde{g} < g_{2n+1}^+ < \cdots < g_3^+ < g_1^+$, that is, $\lim_{n \to \infty} g_{2n}^+ = \lim_{n \to \infty} g_{2n+1}^+ = \widetilde{g}$, so $\widetilde{g}$ is globally asymptotically stable.

Then we prove necessity, and if the assumption does not hold, then there exists at least one $g^* \in [g_p, \widetilde{g})$ such that $P_M^2(g^*) < g^*$. From the stability of periodic solutions and the monotonicity of P_M, it follows that for all $\varepsilon > 0$, there must exist $g_0 \in (\widetilde{g} - \varepsilon, \widetilde{g} + \varepsilon)$ such that $P_M^2(g_0) > g_0$. Since P_M is continuous, there must exist $g_0 \in (\widetilde{g} - \varepsilon, \widetilde{g} + \varepsilon)$ such that $P_M^2(g_0) > g_0$. Since P_M is continuous, there must exist $g_0' \in [g_p, \widetilde{g}]$ such that $P_M^2(g') = g'$, which indicates there exist order-2 periodic solutions for the system, contradicts the global stability of order-1 periodic solutions, so the assumption holds that necessity holds. Where if there are nonnegative integers $m \geqslant 0$ and $k \geqslant 1$ such that k is the smallest integer satisfying $z_m^+ = z_{m+k}^+$ and $T_k = \sum_{i=m}^{m+k-1} \phi(z_i) = \sum_{i=m}^{m+k-1} s_i$, then the locus $\Pi_z \in (X, \Pi, M, I)$ is called order-k periodic solutions $(k = 1, 2, 3, \ldots)$.

When $P_M(g_p) \leqslant g_p$, it can be proved similarly. $\qquad \square$

Theorem 2. *When $\theta\tau > 1$ and $g_A \leqslant g_m$, P_M has the following properties (as shown in Fig. 7(b)):*

  (I) *The domain and range of P_M are $[0, +\infty)$ and N_2, respectively. It is decreasing on the interval $[0, g_p]$ and increasing on the interval $[g_p, +\infty)$; it reaches a minimum at the point g_p. P_M is continuously differentiable over its domain. When $g_k^+ \to +\infty$, it has a horizontal asymptote $g = \tau$.*

  (II) *There is at least one fixed point in P_M as shown in Fig. 7(b). Furthermore, suppose the fixed point is unique. When $P_M(g_p) > g_p$, the fixed point $\widetilde{g}$ is globally stable. When $P_M(g_p) < g_p$, the sufficient condition that for global stability of $\widetilde{g}$ is for all $g^+ \in [g_p, \widetilde{g})$, $P_M^2(g^+) > g^+$.*

Proof. (I) Using the similar argument as in Theorem 1, we can get this conclusion.

(II) For all $g^+ \in [0, +\infty) \setminus N_2$, since $g^+ \in [0, +\infty) \setminus N_2$ is an invariant set of P_M, one obtains $P_M(g^+) \in N_2$. So we can guarantee the existence of the fixed points of model (2) by the continuity, monotonicity, and symptoms of P_M. Denote the unique fixed point by $\widetilde{g}$. If $P_M(g_p) > g_p$, then $\widetilde{g} \in (g_p, +\infty)$ as shown in Fig. 7(b).

When $P_M(g_p) > g_p$, for $g^+ \in (\widetilde{g}, +\infty)$, $\widetilde{g} < P_M(g^+) < g^+$, which is $\widetilde{g} < g_1^+ < g^+$. After n pulse, there is $\widetilde{g} < P_M^n(g^+) < \cdots < P_M(g^+) < g^+$, so $\lim_{n\to\infty} P_M^n(g^+) = \widetilde{g}$. For all $g^+ \in [g_p, \widetilde{g})$, there is $g^+ < P_M(g^+) < \widetilde{g}$, which is $g^+ < g_1^+ < \widetilde{g}$, and after one pulse, there is $P_M(g^+) < P_M(g_1^+) < \widetilde{g}$, which is $g^+ < g_1^+ < g_2^+ < \widetilde{g}$. After n pulses, there is $g^+ < g_1^+ < \cdots < P_M^n(g^+) < \widetilde{g}$, which is $\lim_{n\to\infty} P_M^n(g^+) = \widetilde{g}$. Furthermore, for all $g^+ \in [0, g_p)$, because for all $g^+ \in [0, +\infty)$, there is $P_M(0) = \tau > P_M(g^+)$, which can be discussed in the following three cases: (i) When $P_M(g^+) > \widetilde{g}$, same as $g^+ \in (\widetilde{g}, +\infty)$ after one pulse. (ii) When $g_p \leqslant P_M(g^+) < \widetilde{g}$, after one pulse as in $g^+ \in [g_p, \widetilde{g})$. (iii) $P_M(g^+) = \widetilde{g}, P_M^2(g^+) = \widetilde{g}, \ldots, P_M^n(g^+) = \widetilde{g}$.

Based on the above discussion, it can be concluded that $\widetilde{g}$ is globally stable.

If $P_M(g_p) < g_p$ and the fixed point is unique, we can get that for all $g^+ \in [0, \widetilde{g})$, there is $P_M(g^+) > g^+$, and for all $g^+ \in (\widetilde{g}, +\infty)$, there is $P_M(g^+) < g^+$. $P_M(g^+)$ takes a minimum at g_p, $g_p \in (\widetilde{g}, +\infty)$, $P_M(g^+)$ is decreasing on $g^+ \in (\widetilde{g}, g_p]$.

Analyze the following cases: (i) $g^+ \in (\widetilde{g}, g_p]$; (ii) $g^+ \in [g_p, +\infty)$; (iii) $g^+ \in [0, \widetilde{g})$.

For (i), when $g^+ \in (\widetilde{g}, g_p]$, according to the monotonicity of P_M, we can get $\widetilde{g} > P_M(g^+) \geqslant P_M(g_p)$, and according to the condition $P_M^2(g^+) < g^+$, we can get $\widetilde{g} > P_M^3(g^+) > P_M(g^+)$, which is $P_M(g^+) < P_M^3(g^+) < \widetilde{g} < P_M^2(g^+) < g^+$. After n pulses, according to the mathematical induction method, we can get $P_M(g^+) < P_M^3(g^+) < \cdots < P_M^{2n+1}(g^+) < \widetilde{g} < P_M^{2n}(g^+) < \cdots < P_M^2(g^+) < g^+$. So there are $\lim_{n\to\infty} P_M^{2n}(g^+) = \lim_{n\to\infty} P_M^{2n+1}(g^+) = \widetilde{g}$.

For (ii), when $g^+ \in [g_p, +\infty)$, $P_M^2(g^+) < P_M(g^+), P_M^3(g^+) < P_M^2(g^+)$, so the sequence $P_M^k(g^+)$ is decreasing as k increases, so there exists a positive integer m such that $P_M^m(g^+) \in (\widetilde{g}, g_p]$, as in case (i).

For (iii), there exists an $g_p' \in [0, \widetilde{g})$ such that $P_M(g_p') = g_p$, then for all $g^+ \in [0, g_p')$, after pulsing corresponds to case (ii). For all $g^+ \in [g_p', \widetilde{g}]$, corresponds to case (i) after the pulse, so it is globally stable in case (iii). $\square$

Theorem 3. *When $EP < w_c$, $\theta\tau > 1$, and $g_A > g_m$, P_M has the following properties (as shown in Fig. 7(c)):*

(I) *The domain and range of P_M with value fields $[0, +\infty)$ and N_3, respectively, P_M is continuously differentiable over its domain, and there exists a horizontal asymptote $w = \tau$ for P_M when $g_k^+ \to +\infty$. P_M is decreasing on the interval $g_n^+ \in [0, g_{q1}^+] \cup [g_p, g_{q0}^+]$ and increasing on the interval $g_n^+ \in [g_{q1}^+, g_p] \cup [g_{q0}^+, +\infty)$, reaching a great value at point g_p and a very small value at g_{q1}^+, g_{q0}^+.*

(II) *P_M on N_3 may exist at last one fixed point $\widetilde{g}$ as shown in Fig. 7(c). Especially, suppose the fixed point is unique, there are three cases for its stability as follows: (i) When $P_M(g_{qi}^+) > g_{qi}^+$, $i = 0, 1$, $\widetilde{g}$ is globally stable. (ii) When $P_M(g_{qi}^+) < g_{qi}^+$, $i = 0, 1$, $\widetilde{g}$ is globally stable for all $g^+ \in (\widetilde{g}, g_{q1}^+]$ with $P_M^2(g^+) < g^+$. (iii) If*

$P_M(g_{q1}^+) > g_{q1}^+$ *and* $P_M(g_{q2}^+) < g_{q2}^+$, *then the sufficient condition for the global stability of* $\widetilde{g}$ *is that* $P_M^2(g^+) < g^+$ *holds for all* $g^+ \in (\widetilde{g}, g_{q0}^+]$.

Proof. (I) When $f(g_A) \geqslant \tau$, the phase set is $N_3 = [f(g_m), f(g_A)]$; when $f(g_A) < \tau$, the phase set can also be $N_3 = [f(g_m), \tau]$. In the following, we only need to prove that case (I) is correct when $N_3 = [f(g_m), \tau]$. The other case can be proved similarly. Since $g_A \geqslant g_m$, there exists a unique point $P_0(EP, g_{q0}^+) \in L_4$ and $g_{q0}^+ > g_p$ such that the trajectory from P_0 (denoted ℓ_m) will reach $M(ET, g_m)$ of L_3, and the other intersection of ℓ_m and L_4 is denoted $P_1(EP, y_{q1}^+)$. The same method as in Theorem 2(I) can be used to prove that.

(II) (i) When $P_M(g_{qi}^+) > g_{qi}^+$, we can obtain $\widetilde{g} > g_{q0}^+$, there exists a $g' \in [0, g_{q0}^+)$ making $P_M(g') < \widetilde{g}$. For all $g^+ \in [0, g')$, there is a positive integer m such that $P_m^m(g^+) \in (\widetilde{g}, +\infty)$ and the sequence $P_m^{m+n}(g^+)$ decreases. For all $g^+ \in (g', g_{q0}^+]$, there is a positive integer m such that $P_m^m(g^+) \in (g_{q0}^+, \widetilde{g})$ and the sequence $P_m^{m+n}(g^+)$ increases. So $\lim_{n \to \infty} P_m^l(g^+) = \widetilde{g}$.

(ii) When $P_M(g_{qi}^+) < g_{qi}^+$, $i = 0, 1$, we can get $P_M(g_{qi}^+) < g_{qi}^+$, $i = 0, 1$, and $P_M(g_p) < g_p$ (by the uniqueness of $\widetilde{g}$) for all $g^+ \in (\widetilde{g}, g_{q1}^+]$, by the monotonicity of P_M we can obtain $\widetilde{g} > P_M(g^+) \geqslant P_M(g_{q1}^+)$. From condition $P_M^2(g^+) < g^+$ we get $\widetilde{g} < P_M^2(g^+) < g^+$, after one pulse, we get $\widetilde{g} > P_M^3(g^+) \geqslant P_M(g^+)$, and another pulse, we get $\widetilde{g} < P_M^4(g^+) < P_M^2(g^+) < g^+$, which is $P_M(g^+) < P_M^3(g^+) < \widetilde{g} < P_M^4(g^+) < P_M^2(g^+) < g^+$. After n pulses, there are $P_M(g^+) < \cdots < P_M^{2n-1}(g^+) < \widetilde{g} < P_M^{2n}(g^+) < \cdots < P_M^2(g^+) < g^+$. So there are $\lim_{n \to \infty} P_M^{2n}(g^+) = \lim_{n \to \infty} P_m^{2n-1}(g^+) = \widetilde{g}$. Since $P_m(g_{q0}^+) = P_m(g_{q1}^+)$, so for all $g^+ \in [0, \widetilde{g}) \cup (g_{q1}^+, +\infty)$, there is a positive integer m such that $P_m^m(g^+) \in (\widetilde{g}, g_{q1}^+]$, then the same as $g^+ \in (\widetilde{g}, g_{q0}^+]$, so $\widetilde{g}$ is globally stable.

(iii) When $P_M(g_{q1}^+) > g_{q1}^+$ and $P_M(g_{q2}^+) < g_{q2}^+$, $\widetilde{g} \in (g_{q1}^+, g_{q0}^+)$. For all $g^+ \in (\widetilde{g}, g_{q0}^+]$, there is $\widetilde{g} < g^+ \leqslant g_{q0}^+$. By the monotonicity of P_M we have $\widetilde{g} > P_M(g^+) \geqslant P_M(g_{q0}^+)$. After the pulse, there is $\widetilde{g} < P_M^2(g^+)$, and according to the condition for all $g^+ \in (\widetilde{g}, g_{q0}^+]$, $P_M^2(g^+) < g^+$ holds, which means that $\widetilde{g} < P_M^2(g^+) < g^+$ holds, and after the pulse, there is $\widetilde{g} > P_M^3(g^+) > P_M(g^+)$, which is $P_M(g^+) < P_M^3(g^+) < \widetilde{g} < P_M^2(g^+) < g^+$, so $\lim_{n \to \infty} P_m^{2n}(g^+) = \lim_{n \to \infty} P_m^{2n-1}(g^+) = \widetilde{g}$. For all $g^+ \in [0, \widetilde{g}) \cup (g_{q0}^+, +\infty)$, there is a positive integer m such that $P_m^m(g^+) \in (\widetilde{g}, g_{q0}^+]$, then the situation is the same as above. It can be seen from the above that $\widetilde{g}$ is globally stable. $\qquad \square$

Case (b) in system (2), which has similar properties and proof methods to Theorems 1–3, is omitted here. Next, the dynamic properties of system (2) in case 2 are discussed and summarized as follows.

Theorem 4. *When* $EP \geqslant w_c$ *and* $\theta\tau \leqslant 1$, P_M *has the following properties (as shown in Fig. 8(a):*

(I) *The domains and range of* P_M *are* $[0, g_{T_1}^+] \cup [g_{T_2}^+, +\infty]$ *and* N_4, *respectively.* P_M *is continuously differentiable over its domain. When* $g_k^+ \to +\infty$, *there exists a horizontal asymptote* $g = \tau$ *for* P_M. P_M *is decreasing on* $g_n^+ \in [g_{T_2}^+, +\infty]$

and increasing on $g_n^+ \in [0, g_{T_1}^+]$. Therefore, P_M reaches its maximum value at $g_{T_1}^+, g_{T_2}^+$.

(II) *There may be zero or one fixed point of P_M on N_4 as shown in Fig. 8(a). That is, there may be zero or one order-1 limit cycle of model (2). In particular, suppose that the fixed point is unique when $\widetilde{g} \in [0, g_{T_1}^+]$, then a sufficient condition for the global asymptotic stability of $\widetilde{g}$ is $P_M(g_{T_2}^+) \geqslant g_{T_2}^+$, and $P_M^2(g^+) > g^+$ holds for all $g^+ \in [g_{T_2}^+, \widetilde{g}]$.*

Proof. (I) The property can be proved in a similar way to Theorem 1, and case (II) is discussed below.

(II) For the existence of fixed points, since P_M is decreasing on $g^+ \in [g_{T_2}^+, +\infty)$ and increasing on $g_n^+ \in [0, g_{T_1}^+]$, there is a discontinuity region $(g_{T_1}^+, g_{T_2}^+)$. So when $P_M(g_{T_1}^+) > g_{T_1}^+$ and $P_M(g_{T_2}^+) < g_{T_2}^+$ are satisfied, P_M has no fixed point. Suppose that when $\lim_{g^+ \to g_{T_1}^+} P_M(g^+) < g_{T_1}^+$ and $g^+ < g_{T_1}^+$ hold or $\lim_{g^+ \to g_{T_2}^+} P_M(g^+) > g_{T_2}^+$ and $g^+ > g_{T_2}^+$ hold, there exists at least one fixed point for P_M. In particular, let the fixed point be unique when $g_n^+ \in [0, g_{T_1}^+]$. Then the proof method is similar to that of Theorem 1. When $g^+ \in [g_{T_2}^+, +\infty)$, $P_M(g_{T_2}^+) \geqslant g_{T_2}^+$, so $\widetilde{g} \in [g_{T_2}^+, +\infty)$. For $g^+ \in [g_{T_2}^+, +\infty)$, P_M is decreasing in the interval, and $g^+ < \widetilde{g}$, $P_M(g^+) > \widetilde{g}$ is obtained after pulsing, and $P_M^2(g^+) < \widetilde{g}$ is obtained by pulsing again. According to the conditions, we can obtain $P_M^2(g^+) > g^+$, the synthesis can be obtained $g^+ < P_M^2(g^+) < \widetilde{g}$, after a pulse to get $P_M(g^+) > P_M^3(g^+) > \widetilde{g}$, which is $g^+ < P_M^2(g^+) < \widetilde{g} < P_M^3(g^+) < P_M(g^+) < g^+$. After 2 pulses, we can get $g^+ < P_M^2(g^+) < P_M^4(g^+) < \cdots < P_M^{2n}(g^+) < \widetilde{g} < P_M^{2n-1}(g^+) < \cdots < P_M^3(g^+) < P_M(g^+) < g^+$, that is, $\lim_{n \to \infty} P_M^{2n}(g^+) = \lim_{n \to \infty} P_M^{2n-1}(g^+) = \widetilde{u}$.

That is, $\widetilde{g}$ is globally asymptotically stable. $\qquad \square$

Theorem 5. *When $EP \geqslant w_c$, $\theta\tau > 1$, and $g_T \leqslant g_m$, P_M has the following properties (as shown in Fig. 8(b):*

(I) *The domains and range of P_M are $[0, g_{T_1}^+] \cup [g_{T_2}^+, +\infty]$ and N_5, respectively. P_M is continuously differentiable over its domain. When $g_k^+ \to +\infty$, there exists a horizontal asymptote $g = \tau$ for P_M. P_M is decreasing on $g_n^+ \in [0, g_{T_1}^+]$ and increasing on $g_n^+ \in [g_{T_2}^+, +\infty]$. Therefore, P_M reaches a minimal value at $g_{T_1}^+, g_{T_2}^+$.*

(II) *There may be zero or one fixed point of P_M on N_5 as shown in Fig. 8(b). That is, model (2) may have zero or one order-1 limit cycle. In particular, suppose that the fixed point is unique. When $\widetilde{g} \in [0, g_{T_1}^+]$, the condition for $\widetilde{g}$ to be globally asymptotically stable is $P_M(g_{T_1}^+) \leqslant g_{T_1}^+$; When $\widetilde{g} \in [g_{T_2}^+, +\infty)$, the sufficient condition for global asymptotic stability is $P_M(g_{T_2}^+) \geqslant g_{T_2}^+$, and $P_M^2(g^+) > g^+$ holds for all $g^+ \in [g_{T_2}^+, \widetilde{g}]$.*

Proof. (I) For any points $F_{k_1}^+(EP, g_{k_1}^+)$, $F_{k_2}^+(EP, g_{k_2}^+)$ (here $g_{k_1}^+, g_{k_2}^+ \in [0, g_{T_1}^+]$), let $g_{k_1}^+ < g_{k_2}^+$ and $g_{k+1} = \rho(g_k^+)$. By Cauchy–Lipschitz theorem we can obtain $g_{k_1+1} < g_{k_2+1}$.
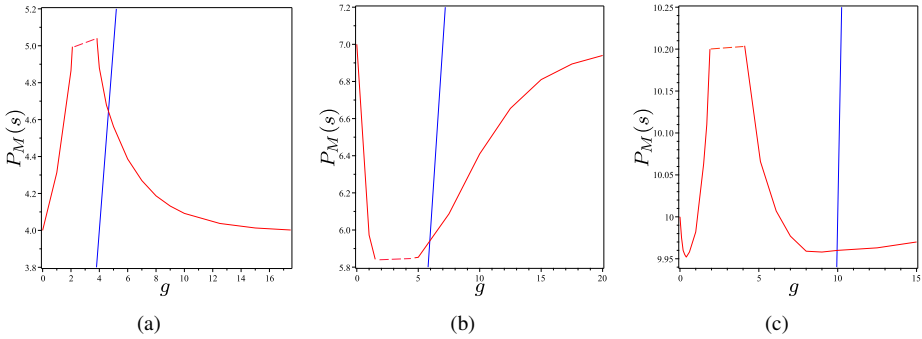
Figure 8. When $EP \geqslant w_c$, the image of P_M with parameters as: $r = 1.5$, $K = 6.8$, $ET = 1.5$, $b = 0.5$, $k = 0.9$, $h = 0.1$, $\sigma = 0.9$, $m = 0.2$, $\tau = 2$, $\theta = 0.4$; (a) $\tau = 4$, $\theta = 0.2$, $d = 0.34$; (b) $\tau = 10$, $\theta = 0.3$, $d = 0.32$; (c) $\tau = 10$, $\theta = 0.11$, $d = 0.32$.

After one pulse, we can obtain $P_M(g_{k_1}^+) = g(ET, g_{k_1}^+) + \tau(1 + \theta g(ET, g_{k_1}^+) > g(ET, g_{k_2}^+) + \tau/(1 + \theta g(ET, g_{k_2}^+)) = P_M(g_{k_2}^+)$.

So P_M is decreasing at $[0, g_{T_1}^+]$.

Similarly, we arbitrarily take two points $Q_{q_1}^+(EP, g_{q_1}^+)$, $Q_{q_2}^+(EP, g_{q_2}^+)$, where $g_{q_1}^+, g_{q_2}^+ \in [g_{T_2}^+, +\infty)$ and set $g_{q_1}^+ < g_{q_2}^+$. The trajectory of $Q_{q_1}^+, Q_{q_2}^+$ will cross L_4 once before reaching L_3 and intersecting L_4 at points $Q_{q_1}{}'(EP, g_{q_1}{}')$, $Q_{q_2}{}'(EP, g_{q_2}{}')$, respectively (here $g_{q_1}{}' > g_{q_2}{}'$). Then each of these two points intersects L_3 at point $Q_{k_1+1}(ET, g_{k_1+1})$, $Q_{k_2+1}(ET, g_{k_2+1})$. According to the Cauchy–Lipschitz theorem, g_{k_1+1}, g_{k_2+1} is obtained reversed (that is, $g_{k_1+1} > g_{k_2+1}$). After pulsing, we get $P_M(g_{q_1}^+) = g(ET, g_{q_1+1}) + \tau/(1 + \theta g(ET, g_{q_1+1})) < g(ET, g_{q_1+2}) + \tau/(1 + \theta g(ET, g_{q_1+2})) = P_M(g_{q_2}^+)$. Therefore, P_M is increasing on $[g_{T_2}^+, +\infty)$ and reaches a minimal value at $g_{T_1}^+, g_{T_2}^+$.

(II) The existence of a fixed point can be proved by a similar method as in the proof of Theorem 1. Moreover, if the fixed point is unique, when $P_M(g_{T_1}^+) \leqslant g_{T_1}^+$, there exists $\widetilde{g} \in (0, g_{T_1}^+]$ such that $P_M(\widetilde{g}) = \widetilde{g}$ holds. For any $g^+ \in [0, \widetilde{g})$, there is $g^+ < P_M(g^+) < \widetilde{g}$. After n pulses, we can get $P_M(g^+) > P_M^2(g^+) > \cdots > P_M^n(g^+) > \widetilde{g}$, which means that there is $\lim_{n \to \infty} P_M^n(g^+) = \widetilde{g}$.

For any $\widetilde{g} \in [\widetilde{g}, g_{T_1}^+)$, there exists $\widetilde{g} < P_M(g^+) < g^+$, and since P_M is decreasing on $[0, g_{T_1}^+]$, there is $\widetilde{g} > P_M^2(g^+) > P_M(g^+)$. After n pulses, there is $\widetilde{g} > P_M^n(g^+) > \cdots > P_M^2(g^+) > P_M(g^+)$, which means that there is $\lim_{n \to \infty} P_M^n(g^+) = \widetilde{g}$. Therefore, $\widetilde{g}$ is globally stable.

When $P_M(g_{T_2}^+) \geqslant g_{T_2}^+$, $\widetilde{g} \in [g_{T_2}^+, +\infty)$, there is $\widetilde{g} \in (g_{T_2}^+, P_M(g_{T_2}^+))$ such that $P_M(\widetilde{g}) = \widetilde{g}$. For any $g^+ \in (g_{T_2}^+, \widetilde{g})$, according to the monotonicity of P_M and the condition $P_M^2(g^+) > g^+$, we can obtain $g^+ < P_M^2(g^+) < \widetilde{g}$. After one pulse, $P_M(g^+) < P_M^3(g^+) < \widetilde{g}$ can be obtained, and after another pulse, $P_M(g^+) < P_M^3(g^+) < \widetilde{g} < P_M^2(g^+) < g^+$ can be obtained. After $2n$ pulses, we can get $P_M(g^+) < P_M^3(g^+) < \cdots < P_M^{2n-1}(g^+) < \widetilde{g} < P_M^{2n}(g^+) < \cdots < P_M^2(g^+) < g^+$, which gives $\lim_{n \to \infty} P_M^{2n}(g^+) = \lim_{n \to \infty} P_M^{2n+1}(g^+) = \widetilde{g}$. Therefore, $\widetilde{g}$ is globally stable. □

Theorem 6. *When $EP \geqslant w_c$, $\theta\tau > 1$, and $g_T > g_m$, P_M has the following properties* (*as shown in Fig. 8(c)*):

(I) *The domains and range of P_M are $[0, g_{T_1}^+] \cup [g_{T_2}^+, +\infty]$ and N_6, respectively. P_M is continuously differentiable over its domain. When $g_k^+ \to +\infty$, there exists a horizontal asymptote $g = \tau$ for P_M. P_M is decreasing on $g_n^+ \in [0, g_{q1}^+] \cup [g_{T_1}^+, g_{q0}^+]$ and increasing on $g_n^+ \in [g_{q1}^+, g_{T_1}^+] \cup [g_{q0}^+, +\infty)$. Therefore, P_M reaches a great value at points g_{T1}^+, g_{T2}^+ and a very small value at g_{q1}^+, g_{q0}^+.*

(II) *There may exist at last one fixed point for P_M on N_6 as shown in Fig. 8(c). That is, system (2) may have at least one limit cycle. If the fixed point is unique, there are three cases for its stability as follows: (i) When $P_M(g_{qi}^+) > g_{qi}^+$, $= 0, 1$, $\widetilde{g}$ is globally stable; (ii) When $P_M(g_{qi}^+) < g_{qi}^+$, $i = 0, 1$, for all $g^+ \in (\widetilde{g}, g_{q1}^+]$ such that $P_M^2(g^+) < g^+$ holds, $\widetilde{g}$ is globally stable. For all $g^+ \in (0, \widetilde{g})$ such that $P_M^2(g^+) > g^+$ holds, $\widetilde{g}$ is globally stable; (iii) If $P_M(g_{q1}^+) > g_{q1}^+$ and $P_M(g_{q2}^+) < g_{q2}^+$ hold, the sufficient condition for $\widetilde{g}$ to be globally stable is that for all $g^+ \in (\widetilde{g}, g_{q0}^+]$, $P_M^2(g^+) < g^+$ holds.*

Proof. Similar to the proof of Theorem 3. □

Case (c) in system (2), which has similar properties and proof methods to Theorems 4–6, is omitted here.

4 Numerical simulations

Figures 9 and 10 are the order-1 periodic solution of system (2) in two cases, respectively. Here the blue line indicates the trajectory after pulse control, and the red line indicates the trajectory without pulse control. The results show that the population density of prey and predator is in a stable range under nonlinear state impulse feedback control. When pulse control is not employed, the number of prey and predators increases for a short period of time and finally drops to very small values. Comparing the prey and predators, they can
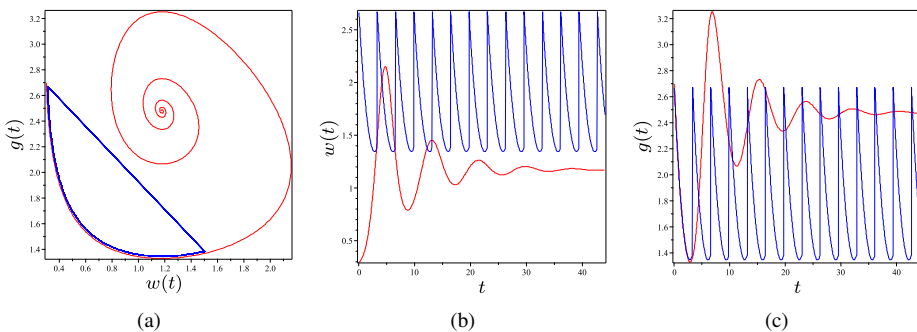

Figure 9. When $\theta\tau \leqslant 1$, the phase diagram and time series of system (2) with parameters as: $r = 1.5$, $K = 6.8$, $ET = 1.5$, $b = 0.5$, $k = 0.9$, $h = 0.1$, $d = 0.5$, $\sigma = 0.9$, $m = 0.2$, $\tau = 2$, $\theta = 0.4$.

survive stably for a long time under effective control. Figure 11 shows that system (2) has an order-1 periodic solution. In Fig. 12, it can be seen that trajectories from different initial points converge to the order-1 periodic solution, which indicates that the order-1 periodic solution is globally asymptotically stable.
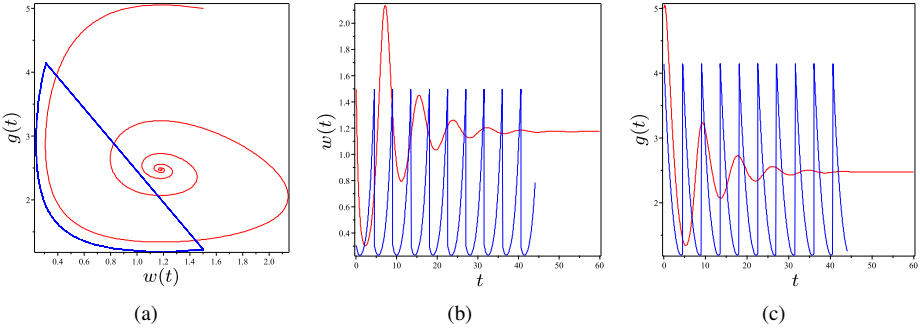

(a) (b) (c)

Figure 10. When $\theta\tau > 1$, the phase diagram and time series of system (2) with parameters as: $r = 1.5$, $K = 6.8$, $ET = 1.5$, $b = 0.5$, $k = 0.9$, $h = 0.1$, $d = 0.5$, $\sigma = 0.9$, $m = 0.2$, $\tau = 7$, $\theta = 0.4$.
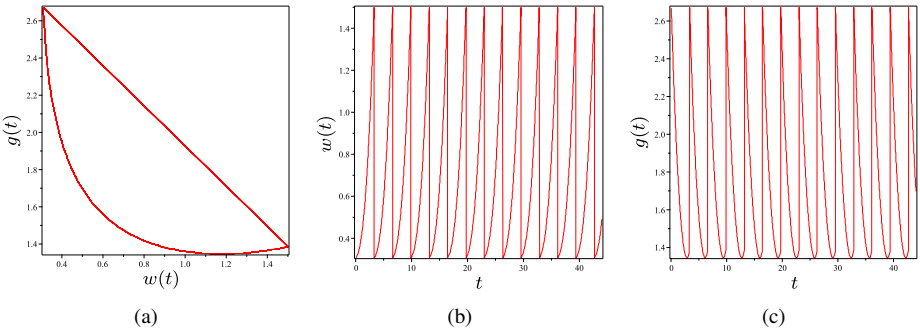

(a) (b) (c)

Figure 11. Periodic solution and time series of system (2) with parameters as: $r = 1.5$, $K = 6.8$, $ET = 1.5$, $b = 0.5$, $k = 0.9$, $h = 0.1$, $d = 0.5$, $\sigma = 0.9$, $m = 0.2$, $\tau = 2$, $\theta = 0.4$.
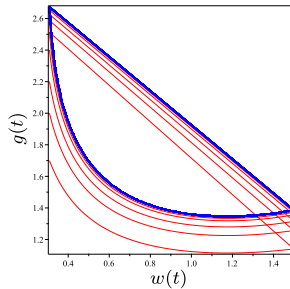

Figure 12. Trajectories of system (2) at different initial points with parameters as: $r = 1.5$, $K = 6.8$, $ET = 1.5$, $b = 0.5$, $k = 0.9$, $h = 0.1$, $d = 0.5$, $\sigma = 0.9$, $m = 0.2$, $\tau = 2$, $\theta = 0.4$.

5 Conclusion

In this paper, we present a predator–prey model with nonlinear state pulse feedback control. The model is constructed considering nonlinear impulse feedback control, which means that the lethality of the prey population and the number of predators released depend on their densities, which makes the model more objective in portraying reality. We mainly discuss the influence of nonlinear state impulse on system dynamics and comprehensively discuss the dynamic properties of system (2). In particular, nonlinear impulse feedback control produces diverse sets of pulses and phases dependent on the parameter space. As a result, the Poincaré map, which is defined on the phase set, changes significantly with the parameter values, for example, producing single-peaked, multi-peaked functions. In particular, discontinuous intervals may appear in the phase set (as shown in Figs. 3 and 5), which gives the Poincaré map a more complex nature. Among other things, the trajectory will have multiple motion scenarios due to the complexity of the parameter space, and the trajectory may experience numerous pulses, finite pulses, or even no pulses at all. Based on this we discuss the properties of the Poincaré map in different cases. In this way, we prove the existence and uniqueness of the order-1 periodic solution of system (2) and give a sufficient condition for the global stabilization of the order-1 periodic solution.

Finally, through numerical simulations, we can see that the nonlinear state pulse control model used in this paper is more consistent with the development of realistic biological populations so that the predator and prey populations can be controlled under the economic threshold ET and the biological populations maintain a stable cyclical and benign developmental change.

Author contributions. All authors have read and approved the final manuscript.

Conflicts of interest. The authors declare that there is no conflict of interest regarding the publication of this paper.

References

1. S. Busenberg, S.K. Kumar, P. Austin, G. Wake, The dynamics of a model of a plankton-nutrient interaction, *Bull. Math. Biol.*, **52**(5):677–696, 1990, `https://doi.org/10.1007/BF02462105`.

2. K. Ciesielski, On stability in impulsive dynamical systems, *Bull. Pol. Acad. Sci., Math.*, **84**(1):81–91, 2004, `https://doi.org/10.4064/ba52-1-9`.

3. T. Daufresne, M. Loreau, Plant–herbivore interactions and ecological stoichiometry: when do herbivores determine plant nutrient limitation?, *Ecol. Lett.*, **4**(3):196–206, 2010, `https://doi.org/10.1046/j.1461-0248.2001.00210.x`.

4. J. Geng, Y. Wang, Y. Liu, L. Yang, J. Yan, Analysis of an avian influenza model with Allee effect and stochasticity, *Int. J. Biomath.*, **16**(06):2250111, 2023, `https://doi.org/10.1142/S179352452250111X`.

5. H. Guo, L. Chen, X. Song, Qualitative analysis of impulsive state feedback control to an algae-fish system with bistable property, *Appl. Math. Comput.*, **271**:905–922, 2015, `https://doi.org/10.1016/j.amc.2015.09.046`.

6. X. Hu, S.R.J. Jang, The role of host refuge and strong Allee effects in a host–parasitoid system, *Int. J. Biomath.*, **16**(05):2250107, 2023, `https://doi.org/10.1142/S1793524522501078`.

7. M. Huang, J. Li, X. Song, H. Guo, Modeling impulsive injections of insulin: Towards artificial pancreas, *SIAM J. Appl. Math.*, **72**(5):1524–1548, 2012, `https://doi.org/10.2307/41698416`.

8. C. Li, Tang S., Analyzing a generalized pest-natural enemy model with nonlinear impulsive control, *Open Math.*, **16**(1):1390–1411, 2018, `https://doi.org/10.1515/math-2018-0114`.

9. H. Li, W. Yang, M. Wei, A. Wang, Dynamics in a diffusive predator–prey system with double Allee effect and modified Leslie–Gower scheme, *Int. J. Biomath.*, **15**(03):2250001, 2022, `https://doi.org/10.1142/S1793524522500012`.

10. B. Liu, Y. Tian, B. Kang, Dynamics on a Holling II predator–prey model with state-dependent impulsive control, *Int. J. Biomath.*, **5**(3):1260006, 2012, `https://doi.org/10.1142/S1793524512600066`.

11. F.R. Musser, M. Kogan, P. Jepson, Perspectives in ecological theory and integrated pest management, *J. Econ. Entomol.*, **102**(4):1726–1727, 2009, `https://doi.org/10.1603/029.102.0445`.

12. L. Nie, J. Peng, Z. Teng, L. Hu, Existence and stability of periodic solution of a Lotka–Volterra predator–prey model with state dependent impulsive effects, *J. Comput. Appl. Math.*, **224**(2):544–555, 2009, `https://doi.org/10.1016/j.cam.2008.05.041`.

13. L. Nie, Z. Teng, Lin H., The dynamics of a chemostal model with state dependent impulsive effects, *Int. J. Bifurcation Chaos*, **21**(5):1311–1322, 2011, `https://doi.org/10.1142/S0218127411029173`.

14. Y. Pei, M. Chen, X. Liang, C. Li, M. Zhu, Optimizing pulse timings and amounts of biological interventions for a pest regulation model, *Nonlinear Anal., Hybrid Syst.*, **27**:353–365, 2018, `https://doi.org/10.1016/j.nahs.2017.10.003`.

15. M.J. Reynolds-Hogland, J.S. Hogland, M.S. Mitchell, Evaluating intercepts from demographic models to understand resource limitation and resource thresholds, *Ecol. Modell.*, **211**(3–4):424–432, 2008, `https://doi.org/10.1016/j.ecolmodel.2007.09.020`.

16. Z. Shi, H. Cheng, Y. Liu, Y. Li, A Cydia Pomonella integrated management predator-prey model with Smith growth and linear feedback control, *IEEE Access*, **7**:126066–126076, 2019, `https://doi.org/10.1109/ACCESS.2019.2938772`.

17. K. Sun, T. Zhang, Y. Tian, Dynamics analysis and control optimization of a pest management predator–prey model with an integrated control strategy, *Appl. Math. Comput.*, **292**:253–271, 2017, `https://doi.org/10.1016/j.amc.2016.07.046`.

18. S. Tang, J. Liang, Y. Tan, R.A. Cheke, Threshold conditions for integrated pest management models with pesticides that have residual effects, *J. Math. Biol.*, **66**(1–2):1–35, 2013, `https://doi.org/10.1007/s00285-011-0501-x`.

19. S. Tang, X. Tan, Y. Jin, J. Liang, Periodic solution bifurcation and spiking dynamics of impacting predator–prey dynamical model, *Int. J. Bifurcation Chaos*, **28**(12):1850147, 2018, `https://doi.org/10.1142/S021812741850147X`.

20. S. Tang, Y. Xiao, R.A. Cheke, Dynamical analysis of plant disease models with cultural control strategies and economic thresholds, *Math. Comput. Simul.*, **80**(5):894–921, 2010, `https://doi.org/10.1016/j.matcom.2009.10.004`.

21. X. Xu, Y. Meng, Y. Shao, Hopf bifurcation of a delayed predator–prey model with Allee effect and anti-predator behavior, *Int. J. Biomath.*, **16**(07), 2023, `https://doi.org/10.1142/S179352452250125X`.

22. Q. Zhang, B. Tang, S. Tang, Vaccination threshold size and backward bifurcation of SIR model with state-dependent pulse control, *J. Theor. Biol.*, **455**:75–85, 2018, `https://doi.org/10.1016/j.jtbi.2018.07.010`.